not only base stacking and hydrogen bonding will be affected by the necessity of making N3 of cytosine and N1 of adenine colinear with Pt will also affect the backbone of DNA. In the latter case coplanarity of the bases may be possible. In addition, distortion may be much less because when platinum replaces the proton, the sugar–sugar distance of 8.65 Å in a Hoogsteen pair[67] is increased to 10.4 Å, which is close to the Watson–Crick distance of 10.8 Å.

A comparison of the model compounds **1** and **5** with the cross-links discussed here suggests that **1** and **5** do not represent "real" models in the sense that the two bases do not adopt a head–head orientation as they do in DNA. Rather, one of the two bases is rotated about the Pt–N bond in order to make a favorable intramolecular hydrogen bond between O2 of cytosine and NH_2 of adenine and to avoid repulsion between the amino groups of both bases.

Acknowledgment. We thank the Deutsche Forschungsgemeinschaft, the National Cancer Institute of Canada, the Natural Sciences and Engineering Research Council of Canada, McMaster University Sciences and Engineering Research Board, and Johnson Matthey Ltd. for financial support.

Supplementary Material Available: Tables of anisotropic temperature factors, perchlorate bond lengths and angles, best planes and dihedral angles, and moduli of F_o and F_c and a figure depicting the chemical shifts as a function of pD (51 pages). Ordering information is given on any current masthead page.

(67) Wang, A. H. J.; Ughetto, G.; Quigley, G. J.; Hakoshima, T.; van der Marel, G. a.; van Boom, J. H.; Rich, A. *Science (Washington, D.C.)* **1984**, *225*, 1115–1121.

Contribution from the Institute of Molecular Physics, Polish Academy of Sciences, 60-179 Poznań, Poland

EPR Spectra of Low-Symmetry Tetrahedral High-Spin Cobalt(II) in a Cinchoninium Tetrachlorocobaltate(II) Dihydrate Single Crystal

H. DRULIS,[1] K. DYREK,[2] K. P. HOFFMANN,[1] S. K. HOFFMANN,* and A. WESEŁUCHA-BIRCZYŃSKA

Received August 13, 1984

EPR spectra of a cinchoninium tetrachlorocobaltate(II) dihydrate [cin$(CoCl_4)\cdot 2H_2O$] single crystal were recorded at 4.2 K. The principal effective g' factors were determined to be $g'_z = 2.13$, $g'_y = 5.57$, and $g'_x = 3.83$ and related to the $\pm^1/_2$ ground state level of the high-spin cobalt(II) in a low-symmetry $CoCl_4^{2-}$ tetrahedron. The true spin-Hamiltonian parameters are $g_\parallel = 2.23$, $g_\perp = 2.38$, and $\lambda = E/D = 0.125$. The relations between g' factors and λ values for several Co(II) tetrahedral complexes are discussed.

Introduction

High-spin tetrahedral Co(II) complexes with different chromophores have been studied by EPR in several crystal lattices.[4-13] EPR results have been described in terms of effective g' factors, which have been interpreted by using the spin-Hamiltonian[11] or/and angular-overlap formalism.[9,13] Hyperfine splitting of ^{59}Co ($I = {}^7/_2$) tends to be relatively small in tetrahedral complexes, is easily smeared out by dipolar and exchange interactions, and thus has been observed only in a few cobalt(II) salts or in magnetically diluted crystals.[4,8]

In regular T_d symmetry the orbital singlet $^4A_2$ is the ground state. When the symmetry is lowered, the spin degeneracy is lifted and either the $\pm^1/_2$ state or the $\pm^3/_2$ state can be lower in energy. The $\pm^1/_2$ state is lower in a flattened tetrahedron, and the $\pm^3/_2$ state is lower in an elongated tetrahedron of D_{2d} symmetry.[9] In most cases, the $\pm^1/_2$ state has been postulated or proved to be the lowest level. The true g-factor values are expected to lie in a range of 2.2–2.7 with $g_\parallel = 2.2$–2.4 in tetrahedral Co(II) complexes.[14] The zero-field splitting $2D$ between $\pm^1/_2$ and $\pm^3/_2$ states in such complexes is found to be rather large, usually of the order of few reciprocal centimeters. For this reason the lowest level is a Kramers doublet and the EPR spectrum can be described in terms of a fictitious spin $S' = {}^1/_2$ using effective g' factors. the g' values are very sensitive to low-symmetry components of the crystal field and thus differ strongly from the true g factors of the Co(II) ions.

In the present paper EPR single-crystal measurements of a low-symmetry $CoCl_4^{2-}$ complex in cin$(CoCl_4)\cdot 2H_2O$ are presented (cin = cinchoninium). The detailed structure of the crystal is not known, but the crystal data of isomorphous cin$(CdCl_4)\cdot 2H_2O$ are available.[15] The stick-bond diagram of the cinchonine molecule is presented in Figure 1. The X-ray data indicate that a series of cinchonine hydrochloride complexes with Cd, Co, Zn, and Hg are isomorphous. The crystals are orthorhombic, with space group $P2_12_12_1$ and $Z = 4$. Tetrahedral $CdCl_4^{2-}$ anions are involved in hydrogen bonds with cinchonine molecules and have essentially C_1 symmetry with Cd–Cl distances in the range 2.42–2.49 Å and bond angles 97.9–117°.

Experimental Section

Preparation of cin$(CoCl_4)\cdot 2H_2O$. The compound was prepared by Dyrek's method.[16] A solution of 10 g of cinchonine ($C_{19}H_{22}N_2O$) in 60

(1) Institute of Low Temperatures and Structural Research, Polish Academy of Sciences, 50-950 Wrocław, Poland.
(2) Department of Chemistry, Jagiellonian University, 30-060 Kraków, Poland.
(3) Regional Laboratory of Physico-Chemical Analysis and Structural Research, Jagiellonian University, 30-060 Kraków, Poland.

(4) Lambe, J.; Baker, J.; Kikuchi, C. *Phys. Rev. Lett.* **1959**, *3*, 270.
(5) van Stapele, R. P.; Beljers, P. F.; Bongers, H. G.; Zijlstra, H. *J. Chem. Phys.* **1966**, *40*, 3719.
(6) Yablokov, Y. V.; Voronkova, V. K.; Shishkov, V. F.; Ablov, A. V.; Veisbein, Z. *Sov. Phys.-Solid State (Engl. Transl.)* **1971**, *13*, 831.
(7) Shankle, G. E.; McElearney, J. N.; Schwartz, R. W.; Kemp, A. R.; Carlin, R. L. *J. Chem. Phys.* **1972**, *56*, 3750.
(8) Guggenberger, L. J.; Prewitt, C. T.; Meakin, P.; Trofimenko, S.; Jesson, J. P. *Inorg. Chem.* **1973**, *12*, 508.
(9) Horrocks, W. D.; Burlone, D. A. *J. Am. Chem. Soc.* **1976**, *98*, 6512.
(10) Bencini, A.; Gatteschi, D. *Inorg. Chem.* **1977**, *16*, 2141.
(11) Pilbrow, J. R. *J. Magn. Reson.* **1978**, *31*, 479.
(12) Bencini, A.; Benelli, C.; Gatteschi, D.; Zanchini, C. *Inorg. Chem.* **1979**, *18*, 2137.
(13) Bencini, A.; Gatteschi, D. *Transition Met. Chem. (N.Y.)* **1982**, *8*, 1.
(14) Jesson, J. P. *J. Chem. Phys.* **1968**, *48*, 161.
(15) Oleksyn, B. J.; Stadnicka, K. M.; Hodorowicz, S. A. *Acta Crystallogr., Sect. B: Struct. Crystallogr. Cryst. Chem.* **1978**, *B34*, 811.
(16) Dyrek, M. *Rocz. Chem.* **1976**, *50*, 2027.

0020-1669/85/1324-4009$01.50/0

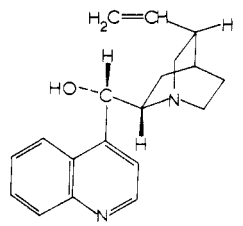

Figure 1. Cinchonine molecule.

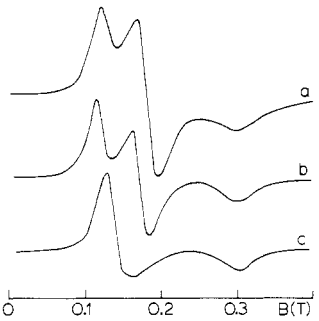

Figure 2. X-Band (9.2 GHz) powder EPR spectra of cin(MCl_4)·$2H_2O$, with M = (Zn,Co) (Zn:Co = 2:1 (a), 100:1 (b)) and M = (Cd,Co) (Cd:Co = 100:1 (c)) recorded at 4.2 K.

mL of HCl (1:1) was mixed with 60 mL of 0.5 M $CoCl_2$. The solution was heated in a water bath for about 1 h until the color changed from pink to dark blue. After it was allowed to cool and stand, the solution deposited well-shaped intensely blue crystals. Mixed crystals (Zn,Co) and (Cd,Co) were obtained by a similar procedure with the ratio of Zn:Co = 2:1 and 100:1 and Cd:Co = 100:1 in the mother solution. All crystals are elongated along the *a* axis with the largest faces (021) and (010) and well-shaped (120) faces. Anal. Calcd for ($C_{19}H_{24}N_2O$)-$CoCl_4$·$2H_2O$: C, 42.80; H, 5.29; N, 5.25; Cl, 26.60; H_2O, 6.76. Found: C, 42.1; H, 5.4; N, 5.3; Cl, 26.6; H_2O, 6.5.[16]

EPR Measurements. EPR spectra of powders and single crystals were recorded on an X-band reflection spectrometer (made by the Technical University of Wrocław, Wrocław, Poland) at 4.2 K. The samples were immersed directly in liquid helium in a Dewar inserted in a cylindrical quartz microwave cavity. Single crystals were rotated in the cavity with respect to the external magnetic field. The magnetic field was calibrated by using an NMR gauss meter. EPR X-band powder spectra were also recorded at 77 K in a liquid-nitrogen insertion Dewar.

Results

The ground state of Co(II) in a tetrahedral environment is the orbital singlet $^4A_2$, but excited orbital levels T_2 and T_1 are relatively close in energy, and in most cases, the spin-relaxation time is very short even at 77 K. As a consequence, powder EPR spectra of cin($CoCl_4$)·$2H_2O$ recorded at liquid-nitrogen temperature consist of a single, asymmetrical broad line centered at about $g' \approx 2.7$ with the peak-to-peak line width of about 150 mT, broader on the side of the higher field. The powder spectra recorded at 4.2 K are shown in Figure 2. The spectra of Co crystals and mixed (Zn,Co) crystals are similar with a small dependence on the Zn:Co ratio. The (Cd,Co) mixed crystals, although displaying a similar $g'_{\parallel}$ value, do not show a splitting in the perpendicular region of the spectra. This is unusual for low-symmetry tetrahedral Co(II) complexes, as will be discussed later. It indicates that an exact isomorphism of Cd and Co or Zn crystals may not occur.

Single-crystal EPR spectra recorded at 4.2 K consist of two resonance lines in all three main crystal planes. This is consistent with the existence of four magnetically nonequivalent $CoCl_4$ tetrahedrons in the crystal unit cell. The line shape is between Gaussian and Lorentzian, and the line width depends on the crystal orientation and varies from 12 to 41 mT. The narrowest lines are observed for minimal g' values, and they are very close to Lorentzian in shape. The broadest lines observed close to the maximal g' values are nearly Gaussian. This suggests that the line shape is at least partially determined by unresolved ^{59}Co hyperfine structure.

The spectra were recorded in the crystal planes *ab*, *bc*, and *ca*, and rotation patterns are presented by points in Figure 3. The

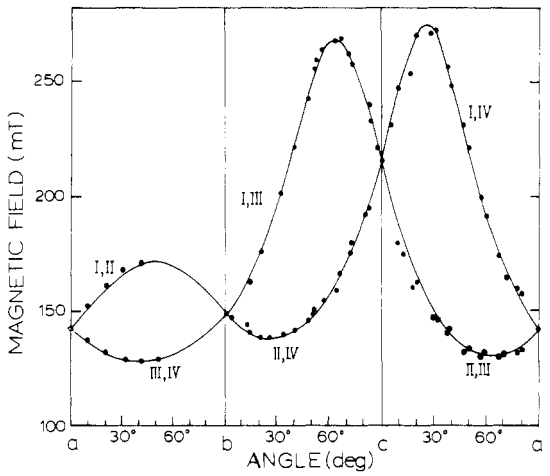

Figure 3. Angular dependence of the EPR resonance field of cin-($CoCl_4$)·$2H_2O$ (X-band, 4.2 K) in *ab*, *bc*, and *ca* crystal planes. The solid lines represent theoretical plots calculated from the data collected in Table I. I, II, III, and IV describe the four magnetically nonequivalent $CoCl_4$ tetrahedrons in the unit cell.

Table I. Effective Principal g' Values and Direction Cosines in the Crystallographic *a*, *b*, *c* Systems[a]

	a	*b*	*c*
$g'_z = 2.13$	0.3156 (+, +, +, +)	0.2839 (+, +, −, −)	0.9054 (−, +, −, +)
$g'_y = 5.57$	0.6891 (+, +, +, +)	0.5883 (+, +, −, −)	0.4232 (+, −, +, −)
$g'_x = 3.83$	0.6659 (+, +, +, +)	0.7454 (−, −, +, +)	0.0302 (−, +, −, +)

[a] The four magnetically nonequivalent $CoCl_4$ complexes are described by subsequent signs of the direction cosines and are denoted by I, II, III, and IV in Figure 3.

data of the *bc* and *ca* planes were least-squares fitted to the equation

$$\mathbf{g}'^2 = \alpha + \beta \cos 2\theta + \gamma \sin 2\theta \qquad (1)$$

and the $\mathbf{g}'^2$-tensor components were calculated by the Waller–Rogers method.[17] Unfortunately, only a part of the data in the *ab* plane was reliable (see Figure 3). Thus it was possible to find all tensor components except g'^2_{ab}. The g'^2_{ab} value was calculated by using powder data. The peak position in the parallel region of the powder spectrum (Figure 2) leads to $g'_z = 2.13$, which has been used for g'^2_{ab} determination. By standard diagonalization procedure the principal g' values and direction cosines of the principal axes were found. Because of an ambiguity in signs of the off-diagonal tensor elements g'^2_{ab}, g'^2_{ac}, and g'^2_{bc} all eight possible sign combinations were considered. Only four of them, I (+++), II (+−−), III (−+−), and IV (−−+), giving an identical set of principal g' values and differing in signs of direction cosines only, reproduce experimental data satisfactorily. The principal g' factors and direction cosines are summarized in Table I. Different signs of direction cosines resulting from I, II, III, and IV are related to the four differently oriented $CoCl_4$ tetrahedrons in the crystal unit cell. The theoretical plots of $B(\theta)$ resulting from the data of Table I for the four magnetically nonequivalent complexes are represented by solid lines in Figure 3.

The data of Table I indicate that the *z* axis of the $CoCl_4$ tetrahedrons form angles of 25° with the crystal *c* axis, and *x* axes lie practically in the crystal *ab* plane, 49° from the *a* axis. The principal axis directions of the effective $\mathbf{g}'^2$ tensor are determined by an interference of the Zeeman and zero-field splitting tensors, and as has been pointed out in ref 10, they are not simply related to the principal axes of either the true $\mathbf{g}^2$ tensor or **D** tensor in the low crystal field symmetry.

(17) Waller, W. G.; Rogers, M. T. *J. Magn. Reson.* **1973**, *9*, 92.

Table II. Effective g' Factors and Nonaxiality Parameters $\lambda = E/D$ for Tetrahedral Cobalt(II) Complexes

no.	compd	chromophore	g'_z	g'_y	g'_x	λ^a	ref
1	$CsCoCl_5$	$CoCl_4$	2.40	4.60	4.60	0	5
2	Cs_2CoCl_4	$CoCl_4$	2.12	5.81	3.39	0.17	9
3	cin($CoCl_4$)·$2H_2O$	$CoCl_4$	2.13	5.57	3.83	0.125	this work
4	$(NEt_4)_2CoCl_4$[b]	$CoCl_4$	3.24	5.44	4.84		7
5	$Co(Ph_3PO)_2Cl_2$[b]	CoO_2Cl_2	2.16	5.67	3.59	0.155	12
6	$Co(py)_2Cl_2$	CoN_2Cl_2	1.77	5.82	2.62	0.27	6, 11
7	$Co(py)_2Br_2$	CoN_2Br_2	2.12	5.48	3.74	0.13	6
8	$Co(\alpha\text{-pic})_2Cl_2$	CoN_2Cl_2	1.50	6.14	2.12	0.33	6, 13
9	$[(n\text{-}C_4H_9)_4N]CoBr_3(quin)$[b]	$CoNBr_3$	1.60	6.31	2.22	0.33	10
10	$Co[H_2B(pz)_2]_2$[b]	CoN_4	6.90	0.95	1.13	0.08[c]	8
11	$Co\{H_2B[3,4,5(CH_3)_3(pz)_2]\}_2$[b]	CoN_4	6.95	0.85	1.02	0.06[c]	8
12	$Co[(C_6H_5)_2B(pz)_2]_2$[b]	CoN_4	7.47	2.28	2.03	0.33[c]	8
13	$Co\{H_2B[3,5(CH_3)_2(pz)_2]_2\}_2$[b]	CoN_4	7.35	2.30	2.00	0.33[c]	8

[a] Calculated from g' values with use of eq 2 and $g_x = g_y = g_\perp$. [b] In isomorphous zinc(II) crystal. [c] λ value estimated from Figure 4.

Discussion

The two-component EPR spectrum of cin($CoCl_4$)·$2H_2O$ indicates that exchange coupling between cobalt(II) ions is very small in the crystal and can be evaluated as $|2J| < 10^{-2}$ cm^{-1}. It is consistent with magnetic susceptibility measurements, which indicate a Curie behavior of χ down to liquid-helium temperature, with $\mu_{eff} = 4.59\ \mu_B$ being in a range typical for high-spin tetrahedral cobalt(II) complexes ($\mu_{eff} = 4.4$–$4.8\ \mu_B$).[18] Thus, effective g' values can be used for calculation of the true molecular g factors of an individual $CoCl_4$ complex in the crystal.

For a large zero-field splitting value ($D \gg h\nu$), as is expected in our crystal, the relation between g' and g values can be found, in first approximation, from the general equation given by Pilbrow (eq 3 in ref 11) as

$$g'_x = g_x[1 \pm (1 - 3\lambda)/M]$$
$$g'_y = g_y[1 \pm (1 + 3\lambda)/M] \qquad g'_z = g_z[1 \pm 2/M] \tag{2}$$

where $\lambda = E/D$ and $M = (1 + 3\lambda^2)^{1/2}$. The upper signs refer to the $\pm^1/_2$ ground level and the lower signs to $\pm^3/_2$. In axial crystal field symmetry $\lambda = 0$, and effective and true g factors are related as $g'_\parallel = -g_z$ and $g'_\perp = 2g_x$ for the $\pm^1/_2$ state and $g'_\parallel = 3g_z$ and $g'_\perp \approx 0$ for the $\pm^3/_2$ state. The axially symmetric effective $\mathbf{g}'^2$ tensors are not commonly found for tetrahedral Co(II) complexes but have been observed for the $CoCl_4$ complex in Cs_3CoCl_5 (Table II).[5] In our case the expected crystal field symmetry of $CoCl_4$ is lower than axial, because of the C_1 geometrical symmetry of the tetrahedron.[15] The tetrahedron deformation results from hydrogen bonds Cl···H–N and Cl···H–O with the cinchonine molecule. Existence of the hydrogen bonds is confirmed by the value of Racah's parameter B resulting from UV–vis measurements, which suggest bonding of the tetrahedron with neighboring molecules.[18] Thus the value of λ differs from zero, and a strongly nonaxial EPR spectrum is observed in our crystal.

The true g factors and nonaxiality parameter λ can be calculated from eq 2 under supposition of axial symmetry of the local $\mathbf{g}^2$ tensors, with $g_x = g_y = g_\perp$ and $g_z = g_\parallel$. The supposition, although not exactly true, can be justified by a small influence of the difference $g_y - g_x$ on the g' values compared to that of λ. The following values were calculated for the $\pm^1/_2$ state as a ground level: $g_\parallel = 2.23$, $g_\perp = 2.38$, and $\lambda = E/D = 0.125$. The values of $g_\parallel$ and $g_\perp$ are in the range expected for tetrahedral Co(II) coordination, and the sequence $g_\parallel < g_\perp$ suggests a flattened tetrahedral structure with the crystal field parameter $Dt < 0$.[9,14] The λ value is one of the smallest among the known values for $CoCl_4$ complexes (see Table II and Figure 4).

Equations 2 indicate that the effective g' parameters are influenced mainly by the value of λ. A deviation of λ from zero results in significant nonaxiality of the effective $\mathbf{g}'^2$ tensor. Thus, in the light of similarity or isomorphism of the Cd(II) and Co(II) cinchonine crystals, a nonaxial EPR spectrum of cobalt(II)-doped cin($CdCl_4$)·$2H_2O$ should appear. The powder spectrum is axial or nearly axial, however (Figure 1), with $g'_\parallel = 2.1$, and $g'_\perp = 4.7$

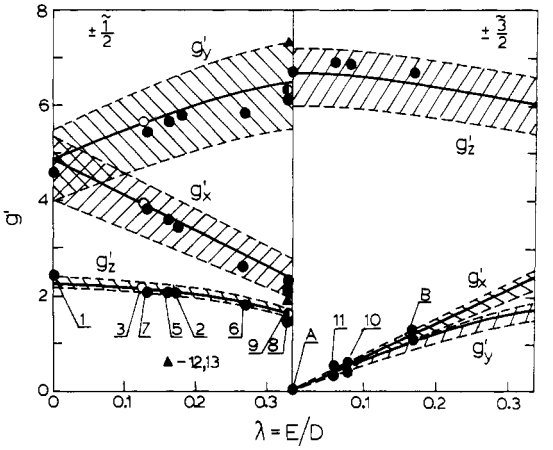

Figure 4. Dependence of effective g' factors on nonaxiality parameter $\lambda = E/D$ for $\pm^1/_2$ and $\pm^3/_2$ ground states. The shadow fields represent possible ranges of g'_i values depending on the true g factors varied in the ranges $g_\parallel = 2.2$–2.4 and $g_\perp = 2.0$–2.7. The lower the true g factor, the lower the g' value. Solid lines represent $g'(\lambda)$ dependences expected for $g_\parallel = 2.23$ and $g_\perp = 2.38$ as have been found in cin($CoCl_4$)·$2H_2O$. The open points indicate position of the cin($CoCl_4$)·$2H_2O$. The black points present results for tetrahedral Co(II) complexes with numbers keyed in Table II. The points A and B represent $\pm^3/_2$ ground-level values of compounds **1** and **2**, respectively.[9]

being the approximately averaged values of g'_x and g'_y for cin($CoCl_4$)·$2H_2O$. One can suggest that either the doped $CoCl_4$ complex is different in structure from the host $CdCl_4$ complex and has an axial symmetry or there exists a physical process resulting in an averaging of the nonaxial components of the $\mathbf{g}'^2$ tensor.

The dominant effect of λ in the determination of the effective g' values, compared to the local g values differentiating CoX_4^{2-} chromophores, suggests a possibility of existence of common features of the $g'(\lambda)$ dependences, independent of the CoX_4^{2-} chemistry. To check this possibility, the EPR data for CoX_4 complexes were summarized in Table II. The λ values for the presented compounds were calculated from eq 2 or were estimated from the theoretical plots presented in Figure 4. The latter has been done for bis[dihydrobis(1-pyrazolyl)borato]cobalt(II) (Co-$[H_2B(pz)_2]_2$) crystals (**10**–**13** in Table II) because of very small nonaxiality of the $\mathbf{g}'^2$ tensors leading the the large influence of the experimental accuracy of g'_x and g'_y on the λ values. The data of Table II are presented by points in Figure 4 together with theoretical g' values predicted from eq 2 for both $\pm^1/_2$ and $\pm^3/_2$ ground-state levels, under the supposition $g_\parallel = 2.2$–2.4 and $g_\perp = 2.0$–2.7 according to Jesson's paper.[14] All the collected compounds, except $(NEt_4)_2CoCl_4$, satisfied the theoretically predicted $g'(\lambda)$ dependence (Figure 4) described by eq 2. Thus, some general conclusions can be drawn, which are practically independent of the details of the CoX_4 chromophore structure.

The expected g' values of the tetrahedrally coordinated Co(II) ions range from 0 to 7. For $\lambda < 0.25$ it is easy to distinguish

(18) Dyrek, K.; Dyrek, M.; Wesełucha-Birczyńska, A. *Polyhedron*, in press.

between $\pm^1/_2$ and $\pm^3/_2$ ground-state levels on the basis of observed g' values. For the $\pm^3/_2$ state the spectra are practically axial in that case, with $g_\perp = 0$–1 and $g_\parallel = 6$–7. For small λ values and $\pm^3/_2$ state, an EPR spectrum can be difficult to detect, since the spectrum would consist of a very small absorption below 100 mT at X-band and a perpendicular peak at very high magnetic field. This situation has been found in bis(*N-tert*-butylpyrrolecarbaldimino)cobalt(II), which at X-band does not show any EPR signal at all.[13] For λ values close to the critical value of $\lambda = {}^1/_3$, it is practically impossible to distinguish between $\pm^1/_2$ and $\pm^3/_2$ states, since in both cases a nearly axial spectrum with $g'_\parallel > g'_\perp$ is expected. The general picture of $g'(\lambda)$ discussed above for Co(II) tetrahedral complexes can be influenced by two factors. Equations 2 are the first approximation of a more general expression, and contributions from higher order terms can be expected,[11] especially in the case of $|2D| < 3$ cm^{-1}. In a low crystal field symmetry a noncollinearity of the $\mathbf{g}^2$ tensor and $\mathbf{D}$ tensor can appear[10] and lead to large variations of apparent g' values, even in the case of a small value of rhombic parameter E.

Acknowledgment. This work was partly carried out under the Project MR I.9.

Registry No. cin($CoCl_4$), 97150-36-2.

Contribution from the Department of Chemistry and Biochemistry, University of California at Los Angeles, Los Angeles, California 90024

Calculation of the Electronic Spectra of Conjugated Cyclic PNS Ring Systems from Preresonance Raman Fundamental and Overtone Intensities

YUN-YEN YANG and JEFFREY I. ZINK*

Received October 26, 1984

Low-temperature electronic absorption spectra and preresonance Raman spectra of $Ph_2PS_2N_3$ (I) and $Ph_4P_2S_2N_4$ (II) are obtained. The absorption spectrum of I exhibits vibronic structure. An overtone in the Raman spectrum of II shows significant intensity. Excited-state distortions of the two compounds are calculated by using the time-dependent theory of electronic and Raman spectroscopy. The electronic absorption spectra are calculated from the Raman-determined data. An excited-state distortion is independently calculated from the overtone intensity in the Raman spectrum. In all cases excellent agreement between experiment and theory is obtained. The distortions of I are compared to those expected from molecular orbital theory.

The time-dependent theory of molecular spectroscopy provides a powerful method for determining excited-state distortions and understanding the details of electronic spectra.[1] It provides both intuitive and quantitative understanding of the connections between preresonance Raman spectroscopy, electronic absorption and emission spectroscopy, and geometry changes between the ground and excited electronic states. The theory has been applied to a limited number of transition-metal,[2,3] organometallic,[4,5] and organic systems.[6]

During the course of our studies of the quantitative relationship between preresonance Raman spectroscopy and electronic spectroscopy, our interest was aroused by the delocalized π systems in inorganic ring compounds. The compounds 5,5-diphenyl-1λ^4,3λ^4,2,4,6,5λ^5-dithiatriazaphosphorine (I) and 5,5,7,7-tetraphenyl-1λ^4,3λ^4,2,4,6,8,5λ^5,7λ^5-dithiatetrazadiphosphocine (II) proved especially useful for study.[7,8] Both compounds have intense

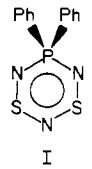

I

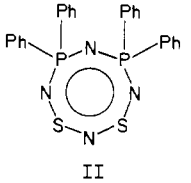

II

electronic transitions in the visible region of the spectrum. As reported below, I exhibits resolved vibronic structure at low temperature and II has significant overtone intensity from a normal mode in its Raman spectrum. These compounds thus provide a test of the applicability of the theory to a previously unstudied type of molecule and electronic transition. In addition, the results provide insight into the electronic structure of this interesting class of molecules. We report here the low-temperature single-crystal electronic absorption spectra, the preresonance Raman spectra, and the quantitative interrelationship between the two in terms of displacements of the excited electronic state along normal coordinates.

Experimental Section

Samples were donated by Prof. Chivers. The techniques for obtaining the low-temperature absorption spectra were described elsewhere.[9] The Raman spectra were recorded by using an RCA C31034-02 phototube, a PAR Model 1105 photon counter, and a Spex 1401 monochromator. Excitation radiation was provided by a Spectra Physics argon ion laser and a krypton ion laser. The monochrometer and photon counter were controlled by a PDP 11/02 computer. The Raman spectra were collected and stored digitally.

Theory

The time-dependent theory of molecular spectroscopy provides both a quantitative and an intuitive physical picture of the interrelationship between preresonance Raman spectra and electronic absorption spectra.[1] In both types of spectroscopy, the spectra are governed by the motion of a wave packet on a multidimensional excited-electronic-state potential hypersurface. A cross section of the multidimensional surface along one normal mode, which will be used to discuss the theory, is shown in Figure 1.

The absorption process according to time-dependent theory[10] is illustrated on the left side of Figure 1. The initial vibrational wave packet, ϕ, propagates on the upper potential surface, which, in general, is displaced relative to the ground surface. The displaced wave packet is not a stationary state and evolves according

(1) Heller, E. J. *Acc. Chem. Res.* **1981**, *14*, 368-375.
(2) Yang, Y. Y.; Zink, J. I. *J. Am. Chem. Soc.* **1984**, *106*, 1500-1501.
(3) Yoo, C. S.; Zink, J. I. *Inorg. Chem.* **1983**, *22*, 2476-2477.
(4) Tutt, L.; Tannor, D.; Schindler, J.; Heller, E. J.; Zink, J. I. *J. Phys. Chem.* **1983**, *87*, 3017-3018.
(5) Tutt, L.; Tannor, D.; Heller, E. J.; Zink, J. I. *Inorg. Chem.* **1982**, *21*, 3859.
(6) Myers, A. B.; Mathies, R. A.; Tannor, D. J.; Heller, E. J. *J. Chem. Phys.* **1982**, *77*, 3857-3866.
(7) Burford, N.; Chivers, T.; Cordes, A. W.; Laidlaw, W. G.; Noble, M. C.; Oakley, R. T.; Swepton, P. N. *J. Am. Chem. Soc.* **1982**, *104*, 1282-1290.
(8) Burford, N.; Chivers, T.; Richardson, J. F. Inorg. *Chem.* **1983**, *22*, 1482-1487.
(9) Chang, T. H.; Zink, J. I. *J. Am. Chem. Soc.* **1984**, *106*, 287.
(10) Heller, E. J. *J. Chem. Phys.* **1978**, *68*, 3891-3896.

0020-1669/85/1324-4012$01.50/0